ARTICLE
Journal of Cellular Biochemistry 115:928–939 (2014)

Journal of Cellular Biochemistry

High Glucose Condition Suppresses Neurosphere Formation by Human Periodontal Ligament-Derived Mesenchymal Stem Cells

Chenphop Sawangmake,[1,2,3] Prasit Pavasant,[2,4] Piyarat Chansiripornchai,[1] and Thanaphum Osathanon[4,5]*

[1]*Department of Pharmacology, Faculty of Veterinary Science, Chulalongkorn University, Bangkok 10330, Thailand*
[2]*Research Unit of Mineralized Tissue, Faculty of Dentistry, Chulalongkorn University, Bangkok 10330, Thailand*
[3]*Graduate Program in Veterinary Bioscience, Faculty of Veterinary Science, Chulalongkorn University, Bangkok 10330, Thailand*
[4]*Department of Anatomy, Faculty of Dentistry, Chulalongkorn University, Bangkok 10330, Thailand*
[5]*DRU in Genetic and Anatomical Analyses of Craniofacial Structure, Faculty of Dentistry, Chulalongkorn University, Bangkok 10330, Thailand*

ABSTRACT

D-Glucose serves many roles in cellular functions, but its role in human periodontal ligament-derived mesenchymal stem cells (hPSLSCs) is yet unknown. Here, the roles of high glucose concentration on neurogenic differentiation by hPDLSCs were investigated. Two-stage neurogenic induction protocol was employed. Cells were maintained in normal neurogenic induction medium, high glucose condition, or high mannose condition. The results showed that high glucose attenuated neurosphere formation efficiency by hPDLSCs in terms of morphology, neurogenic marker expression, without a deleterious effect on cell viability. Contrastingly, neurosphere-derived cells matured in high glucose condition exhibited normal neuronal characteristics compared to the control. During neurosphere formation in high glucose, glucose transporters (GLUTs) mRNA levels were significantly decreased, corresponding with the deprivation of cellular glucose uptake. Further, a glucose uptake inhibitor, cytochalasin B, was used to confirm the deleterious effects of glucose uptake deprivation during neurosphere formation. The results demonstrated that deprivation of glucose uptake attenuated neurosphere formation efficiency by hPDLSCs. Together, the results illustrated that high glucose condition attenuated the efficiency of neurosphere formation but not neuronal maturation, which may occur through the downregulation of *GLUTs* and the reduction of glucose uptake. J. Cell. Biochem. 115: 928–939, 2014.

KEY WORDS: PERIODONTAL LIGAMENT-DERIVED MESENCHYMAL STEM CELLS (hPDLSCs); GLUCOSE; NEURONAL DIFFERENTIATION

Periodontal ligament provides tooth support and serves as cell resources for alveolar bone and periodontal tissue regeneration [Song et al., 2012]. Various cell types reside in periodontal ligament, including vascular endothelial cells, smooth muscle cells and fibroblast cells [Song et al., 2012]. Interestingly, several publications suggested the stem cell-liked properties of periodontal ligament-derived subpopulation. Those cells contain self-renewal ability and multipotential differentiation capability. The examples are neurons, hepatocytes, osteoblasts, chondrocytes, and adipocytes [Seo et al., 2004; Grimm et al., 2011; Egusa et al., 2012; Osathanon et al., 2013b]. Moreover, the expression of mesenchymal stem cell markers (STRO-1, CD-44, CD-73, CD-90, and CD-105) and embryonic

Conflict of Interest: The authors indicate no potential conflicts of interest.

Grant sponsor: Ratchadapiseksomphot Endowment Fund of Chulalongkorn University; Grant number: RES560530156-HR; Grant sponsor: Chulalongkorn University Graduate Scholarship to Commemorate the 72nd anniversary of His Majesty King Bhumibol Adulyadej; Grant sponsor: Government Research Fund; Grant sponsor: 2012 Research Chair Grant, Thailand National Science and Technology Development Agency (NSTDA), Thailand; Grant sponsor: Thailand Research Fund (Royal Golden Jubilee Scholarship).

*Correspondence to: Assistant Professor Thanaphum Osathanon, DDS, PhD, Department of Anatomy, Faculty of Dentistry, Chulalongkorn University, Henri-Dunant Rd., Pathumwan, Bangkok 10330, Thailand. E-mail: osathanon.t@gmail.com

Manuscript Received: 9 April 2013; Manuscript Accepted: 4 December 2013

Accepted manuscript online in Wiley Online Library (wileyonlinelibrary.com): 16 December 2013

DOI 10.1002/jcb.24735 • © 2013 Wiley Periodicals, Inc.

stem (ES) cell markers (OCT-4, NANOG, SOX-2, REX-1, SSEA-1, SSEA-3, SSEA-4, TRA-1–60, and TRA-1–81) has also been reported, suggesting the stem cell characteristics of human periodontal ligament stem cells (hPDLSCs) [Kadar et al., 2009; Kawanabe et al., 2010; Mrozik et al., 2010].

In the regard of neuronal differentiation, many publications have been reported on the successes of in vitro formation of neuronal lineage cells from PDLSCs [Kadar et al., 2009; Li et al., 2010; Mi et al., 2011; Osathanon et al., 2013b]. By two-step neuro-induction protocol, the spindle-shape cells with long neurite-like extensions along with neurogenic marker upregulation have been successfully produced from PDLSCs in vitro [Techawattanawisal et al., 2007; Osathanon et al., 2013a,b]. This protocol consists of neuroprogenitor (neurosphere) formation and neuronal maturation step. Regardless, several factors have been shown to involve and regulate neurogenic differentiation by various types of stem and progenitor cells. The regulation might also be cell type specific. In this regards, an experiment conducted under in vitro oxygen-glucose deprivation (OGD) condition has suggested the sensitivity of developing or immature hippocampal neurons [Jiang et al., 2004]. Moreover, glucose reduction could prevent replicative senescence and increase mitochondrial respiration by human mesenchymal stem cells, suggesting the importance and relevance of glucose on cell function and viability [Lo et al., 2011].

D-Glucose, an aldohexose sugar, serves a pivotal role in cell function and respiration. Metabolism of glucose provides energy-supplying molecules and many metabolic intermediates, which are important to cell function [Maciver et al., 2008]. The optimal glucose conditions have been studied and used for stem cell maintenance and differentiation. In this respect, inducing condition supplied with 25 mM glucose could enhance the efficiency of cardiogenic differentiation, but inhibit the propensity of neurogenic differentiation by embryoid body (EB) derived from mouse ES cells [Mochizuki et al., 2011]. Contrastingly, three different glucose conditions (5.5, 25, and 45 mM) were able to support mouse ES cell-derived EB formation in similar appearances and pluripotent marker patterns [Mochizuki et al., 2011]. These results suggested the variety of cellular responses toward glucose conditions. However, the study and evidence regarding glucose effects on neuronal differentiation by hPDLSCs are yet unknown. Thus, the objective of this study was pointed out to explore the effect and relevance of glucose conditions on in vitro differentiation of hPDLSCs toward neurogenic lineage.

MATERIALS AND METHODS

hPDLSCs ISOLATION AND CULTURE

The hPDLSCs were isolated and cultured following the previous published protocol [Osathanon et al., 2013a]. Protocols were approved by the Ethical Committee, Faculty of Dentistry, Chulalongkorn University. Teeth removal due to impaction and orthodontic reasons were collected for cell isolation. The donor teeth must contain no caries, no inflammation, or other pathological conditions. The isolated cells were maintained at 37°C, 100% humidified and 5% carbondioxide condition. Dubecco′s modified Eagle medium (DMEM with 4.5 g/L glucose; Gibco) supplemented with 10% FBS (Gibco), 2 mM L-glutamine (Gibco), 100 U/ml penicillin (Gibco), 100 μg/ml streptomycin (Gibco), and 5 μg/ml amphotericin B (Gibco) was used as the culture medium and changed every 48 h.

hPDLSCs CHARACTERIZATION

The isolated cells were characterized by using reverse transcription-polymerase chain reaction (RT-PCR) and flow cytometry. Expressions of transcription factors identifying stemness properties (*REX-1*, *NANOG*, and *OCT-4*) and surface markers (CD24, CD44, CD45, CD73, CD90, CD105, and STRO-1) were evaluated. Further, the multipotential differentiation properties regarding osteogenic and adipogenic lineages were investigated. The characterization protocols were performed according to our previous reports [Govitvattana et al., 2013; Nowwarote et al., 2013]. Briefly, for osteogenic induction, hPDLSCs were seeded into 24-well plate in a concentration of 2.5×10^4 cells/well. Cells were maintained in osteogenic induction medium for 14 days with every 48-h substitution. Osteogenic medium was growth medium supplemented with 50 μg/ml ascorbic acid, 100 nM dexamethasone, and 10 mM β-glycerophosphate. Regarding adipogenic induction, cells were plated into 24-well plate and maintained with adipogenic induction medium supplemented with 0.1 mg/ml insulin, 1 μM dexamethasone, 1 mM IBMX, and 0.2 mM indomethacin for 16 days.

NEUROGENIC DIFFERENTIATION

Two-step induction protocol that comprises neuroprogenitor (neurosphere) formation and neuronal cell maturation was used to induce neurogenic differentiation of hPDLSCs [Osathanon et al., 2013a]. In summary, during the first 7 days, hPDLSCs were seeded in 60-mm-Petri dishes (Falcon) and supplemented with neuroinduction medium. Then, hPDLSCs-derived neurospheres were transferred into collagen type IV (Sigma)-coated culture dishes (Corning) and grown with neuroinduction medium supplemented with retinoic acid (Sigma) for another 7 days. Neurobasal medium (Gibco) supplemented with 20 ng/ml bFGF (Invitrogen), 20 ng/ml EGF (Sigma), 2 μg/ml heparin (Sigma), 1% serum free B-27 supplement (Invitrogen), 2 mM L-glutamine, 100 U/ml penicillin, 100 μg/ml streptomycin, and 5 μg/ml amphotericin B was used as the neuroinduction medium and changed every 48 h. To explore the roles of glucose conditions on neurogenic differentiation by hPDLSCs, 18 g/L D-glucose (Sigma) was added into neurobasal medium (4.5 g/L glucose) in order to make 22.5 g/L (5×)-glucose neuroinduction medium. D-mannose (Sigma) at the same concentration was used as the control to compare and elucidate the effects of increased neuroinduction medium osmolarity. In some experiments, cytochalasin B (10 μM), a glucose uptake inhibitor, was used to elucidate the effects of glucose uptake deprivation during neurosphere formation. Data were collected at days 1, 3, and 7 in each step of neuroinduction. Neurospheres and mature neuronal cells were captures and analyzed for sizes and spreading diameters by using of AxioVision Rel. 4.8 program. Reverse transcription-polymerase chain reaction (RT-PCR) was used to evaluate the mRNA expressions. Immunocytochemistry was used to confirm the expression of βIII-TUBULIN (βIII-T) at protein level. Fluorescent glucose-uptake cell-based assay was performed to verify the intracellular glucose. Calcein AM and EthD-1 were used to determine cell viability.

RT-PCR

The cellular RNA was extracted with Trizol reagent. Then, RNA samples (1 μg) were converted to cDNA using reverse transcriptase enzyme kit (Promega). Taq polymerase enzyme kit (Invitrogen) was used to amplify the target genes. Amplified cDNA was electrophoresed on 1.8% agarose gel and stained with ethidium bromide. The18S ribosomal RNA was used as a reference gene. For real time quantitative RT-PCR (qRT-PCR), LightCycler®480 SYBR Green I Master kit (Roche Diagnostic) was employed. The mRNA expression was normalized to 18S and then further normalized to the control. The primer sequences were shown in Supplementary Table SI.

FLOW CYTOMETRY

The hPDLSCs were stained with PE-conjugated anti-CD24 antibody (BD Biosciences Pharmingen), FITC-conjugated anti-CD44 antibody (BD Biosciences Pharmingen), PerCP-conjugated anti-CD45 antibody (BD Biosciences Pharmingen), PerCP-Cy™5.5-conjugated anti-CD90 antibody (BD Biosciences Pharmingen), and PE-conjugatd anti-CD105 antibody (BD Biosciences Pharmingen). For data analysis, FACSCalibur regarding the CellQuest software (BD Bioscience) was used, and values were illustrated as mean fluorescence intensity (MFI).

IMMUNOCYTOCHEMISTRY STAINING

Neurospheres and neuronal cells attached on collagen IV-coated plates were fixed in cold methanol for 15 min, then permeabilized with 0.1% Triton®-X100 in PBS for 1 min, and incubated with 10% horse serum in PBS for 1 h. Primary antibody, mouse anti-βIII-TUBULIN (Promega), was used to incubate at 1:100 dilution for 18 h. After that, biotinylated-goat anti-mouse antibody (1:500 dilution; Invitrogen) and streptavidin-FITC (1:500 dilution; Sigma) were used to incubate for 1 h in each step. DAPI (0.1 μg/ml) was used for nuclei counterstaining. All of procedures were performed at 4°C and washed with PBS in every step. The results were analyzed by fluorescent microscope incorporated with Carl Zeiss™ Apotome.2 apparatus (Carl Zeiss, Germany).

GLUCOSE UPTAKE CELL-BASED ASSAY

Glucose uptake by neurospheres and neuronal cells were explored by glucose uptake cell-based assay kit (Cayman chemical). Briefly, cells were incubated with glucose-free medium containing 200 μg/ml 2-NBDG (2-deoxy-2-[(7-nitro-2,1,3-benzoxadiazol-4-yl)amino]-D-glucose) for 10 minutes at 37°C, then washed with warm cell-based assay buffer and immediately analyzed by fluorescent microscope incorporated with Carl Zeiss™ Apotome.2 apparatus.

CELL VIABILITY ASSAY

Live/Dead® cell viability assay (Invitrogen) was used to assess the cell viability. In summary, neurospheres and neuronal cells were stained with calcein acetoxymethyl ester (calcein AM) and ethidium homodimer-1 (EthD-1) at 37°C for 15 min. The stained cells were then washed with warm PBS and analyzed by flow cytometer and fluorescent microscope incorporated with Carl Zeiss™ Apotome.2 apparatus. For flow cytometry, the single cell suspension was obtained before staining. In some experiments, MTT assay was employed. Briefly, cells were incubated in MTT solution for 15 min and then the formazan crystals were solubilized using glycine-dimethylsulfoxide buffer for absorbance measurement at 570 nm.

STATISTICAL ANALYSES

The results were showed as mean ± standard deviation (SD). Data were analyzed using one-sample *t*-test for determining difference within one group or independent Student's *t*-test for two sample groups or one-way analysis of variance (ANOVA) followed by Dunnett post hoc for three or more sample groups. Three subjects ($n = 3$) were used in the study. Significant difference was recognized when P-value <0.05.

RESULTS

hPDLSCs CHARACTERIZATION

The isolated cells were characterized for the stem cell characteristics using RT-PCR, flow cytometry (Fig. 1A,B), and immunocytochemistry

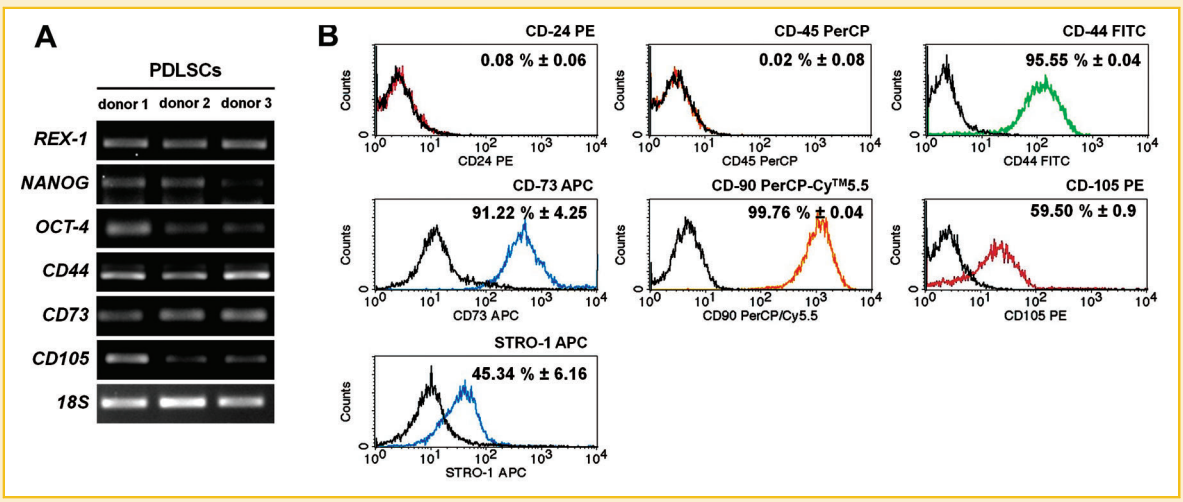

Fig. 1. hPDLSCs characterization. Transcription factors identifying stemness properties (i.e., REX-1, NANOG, and OCT-4) and surface markers (i.e., CD24, CD44, CD45, CD73, CD90, CD105, and STRO-1) were analyzed using RT-PCR (A) and flow cytometry (B).

staining (Supplementary Fig. S1). The expression of transcription factors identifying stemness properties including *REX-1*, *NANOG*, and *OCT-4* were illustrated. Moreover, surface markers of mesenchymal stem cells (CD44, CD73, CD90, CD105, and STRO-1) were also expressed, while hematopoietic related surface markers (CD24 and CD45) were not detected. There is no statistical significant different among three individuals on the surface marker expression. In order to clarify the multipotential differentiation properties of established hPDLSCs, cellular differentiation toward osteogenic and adipogenic lineages was employed. By culturing cells in osteogenic induction medium, hPDLSCs were able to differentiate into osteogenic lineage (Fig. 2A), confirming by the dramatic increase of mineral deposition and the upregulation of osteogenic marker gene expression (*COLLAGEN I* [*COL I*] and *OSTEOCALCIN* [*OCN*]) at day 14. A significant increase of alkaline phosphatase (ALP) activity was shown at day 7. Moreover, the intracellular lipid droplets were noted upon maintained cells in adipogenic induction medium for 16 days, corresponding with the increase of adipogenic marker mRNA

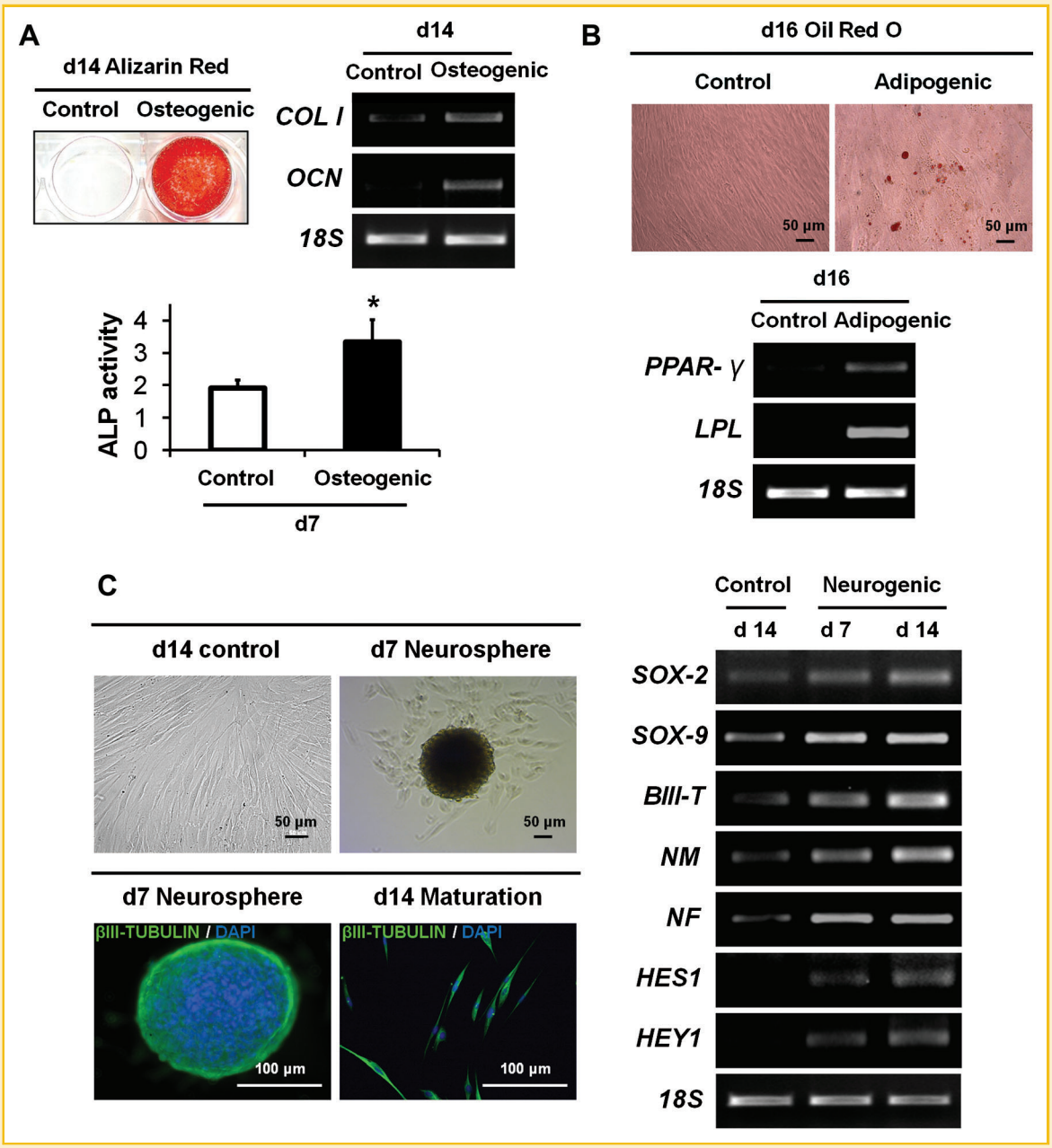

Fig. 2. Multipotential differentiation capability and neuronal differentiation of hPDLSCs. For osteogenic differentiation, the increase of mineral deposition, osteogenic marker gene expression, and alkaline phosphatase enzymatic activity was illustrated (A). Regarding adipogenic induction (B), the intracellular lipid accumulation and adipogenic marker gene expression were demonstrated using oil red O staining and RT-PCR, respectively. For neuronal differentiation (C), the neurosphere formation was observed and the βIII-TUBULIN expression was illustrated in the spheres and attached differentiated cells. Neurogenic marker gene expression was analyzed by RT-PCR. Asterisks indicated the statistical significance compared to the control.

expression (*PEROXISOME PROLIFERATOR–ACTIVATED RECEPTOR-GAMMA* [*PPAR-γ*] and *LIPOPROTEIN LIPASE* [*LPL*]) (Fig. 2B).

DIFFERENTIATION OF hPDLSCs TOWARD NEURONAL LINEAGE

Neurosphere formation technique as described in our previous report was used to differentiate hPDLSCs into neuronal lineage [Osathanon et al., 2011, 2013a]. The hPDLSCs seeded in 60-mm-Petri dishes and supplemented with neuroinduction medium were able to form neurosphere (neuroprogenitor) since day 1 (data not shown) and the average size of sphere at day 7 was 150.49 ± 79.79 μm in diameter (Fig. 2C). Further, hPDLSCs-derived neurospheres were transferred into collagen type IV-coated culture dishes and maintained in neuroinduction medium supplemented with retinoic acid for another 7 days to let the cell migrate and mature. At day 14, neurosphere-derived cells migrated out and attached to the culture dish. Those cells exhibited long, thin neurite-like extension processes. Both day 7 neurosphere and day 14 mature neuronal cells expressed βIII-TUBULIN protein as observed by immunocytochemistry staining. The upregulation of neurogenic gene markers (*SOX-2*, *SOX-9*, *βIII-T*, *NEUROMODULIN* [*NM*], and *NEUROFILAMENT* [*NF*]) was noted. Moreover, Notch target genes, *HES1* and *HEY1*, were upregulated, suggesting the involvement of Notch signaling in neurogenic differentiation of hPDLSCs as described in our previous publication [Osathanon et al., 2013a]. Together, the results suggested the capability of hPDLSCs differentiation toward neuronal lineage.

HIGH GLUCOSE CONDITION SUPPRESSED NEUROSPHERE FORMATION BY hPDLSCs

To examine the roles of high glucose conditions on hPDLSCs, D-glucose was added into culture medium to make 2× (9 g/L), 5× (22.5 g/L), and 10× (45 g/L) glucose concentration (Supplementary Fig. S2). At high glucose condition (10×), the abnormal cell morphology was noted and appeared in round shape and floating, implying cell death. Therefore, two glucose conditions were further employed in neurogenic induction. However, there is no obvious difference in the sphere's size in 2× glucose condition. Thus, the 5× glucose concentration was utilized in further experiments. D-Mannose at the same concentration was used to elucidate the effects of increased osmolarity. The normal neuroinduction medium was employed as the control. The physical properties of neurogenic media, including density and viscosity were tested. The results revealed no significant difference of those physical properties among three different culture mediums (data not shown). In addition, there was no significant difference in cell number at days 1, 3, and 7 upon maintaining hPDLSCs in all three culture condition (normal, 5× glucose, and mannose) as determined by MTT assay, suggesting no influence of culture condition on cell toxicity and proliferation (data not shown).

In neurosphere formation with high glucose neurogenic medium (Neuro + Glu), the hPDLSCs-derived neurospheres appeared smaller in size than normal neurogenic induction medium (Neuro; Fig. 3A). The average sphere size was not significantly different (Supplementary Fig. S3). However, a trend of an increased percentage of small-size neurosphere (<50 μm) was found in high glucose group (Fig. 3B). For high mannose group (Neuro + Man), the trend of the neurosphere's size was slightly smaller than the control, but there was still larger than high glucose group. Additionally, neurogenic gene markers (*SOX-2*, *SOX-9*, *βIII-T*, *NM*, and *NF*) and Notch target genes (*HES1* and *HEY1*) of neurospheres derived from high glucose group were downregulated and the significant difference was found in *SOX-2*, *HES1*, and *HEY1* compared to the control. The expression levels in mannose group exhibited in similar levels to the control (Fig. 3C). Moreover, the βIII-TUBULIN protein expression in high glucose condition was apparently decreased comparing with neurospheres from the control and high mannose group as seen by immunocytochemistry staining (Fig. 3D).

The glucose transporters (*GLUTs*) mRNA expression was evaluated at day 7. The results demonstrated the downregulation of *GLUT1*, *GLUT2*, and *GLUT3* mRNA expression in high glucose condition compared to the control (Fig. 3E). However, the significant difference was noted in *GLUT2*, and *GLUT3*. The *GLUTS* mRNA expression in high mannose group exhibited in similar levels to the control. Further, a glucose uptake cell-based assay using fluorescent glucose analogue, 2-NBDG, was employed. The high glucose-derived neurospheres showed a relative decreased intracellular glucose compared to the control and high mannose group, suggesting the lower ability to uptake glucose into the cells (Fig. 3F). Moreover, cell viability was evaluated using Calcein AM and ethidium homodimer-1. By analyzing with fluorescence microscope, most of cells in three conditions were stained with green fluorescence of Calcein AM suggesting the cell viability (Fig. 3G). Moreover, flow cytometry analysis revealed no significant difference in cell viability among three conditions, thus, excluding the potential influence of cell death on the observed phenomenon (Fig. 3H). Together, the results illustrated the defects of neurosphere formation upon high glucose condition, and the downregulation of *GLUTs* along with a decreased glucose uptake were concurrently occurred.

NORMAL hPDLSCs–DERIVED NEUROSPHERES UNDERWENT NEURONAL MATURATION EVEN IN HIGH GLUCOSE CONDITION

Further investigations regarding the ability of neurosphere maturation in high glucose condition were investigated. The hPDLSCs-derived neurospheres obtained from normal induction protocol were used. The spheres were seeded into collagen IV-coated culture dishes and maintained in neurogenic medium supplemented with retinoic acid for another 7 days. The collagen IV-attached spheres were further maintained in three different culture conditions; the normal neurogenic medium control, high glucose medium and high mannose medium. There was no difference in sphere size, morphology, and cell migration upon seeding on collagen IV in all medium conditions (Fig. 4A,B). Moreover, the neurogenic marker genes were exhibited in similar levels. No statistical significance was noted among three culture conditions (Fig. 4C). In addition, no obvious change was noted in regard of the βIII-TUBULIN protein expression at day 7 in all those culture condition (Fig. 4D). Further, there was no significant difference in *GLUT* mRNA expression, glucose uptake efficiency, as well as cell viability among those conditions (Fig. 4E–H). Together, the results suggest that high glucose condition does not influence the maturation process of hPDLSCs-derived neurospheres.

CYTOCHALASIN B ATTENUATED NEUROSPHERE FORMATION BY hPDLSCs

As described above, high glucose condition attenuated neurosphere formation by hPDLSCs. This was concurrently with the

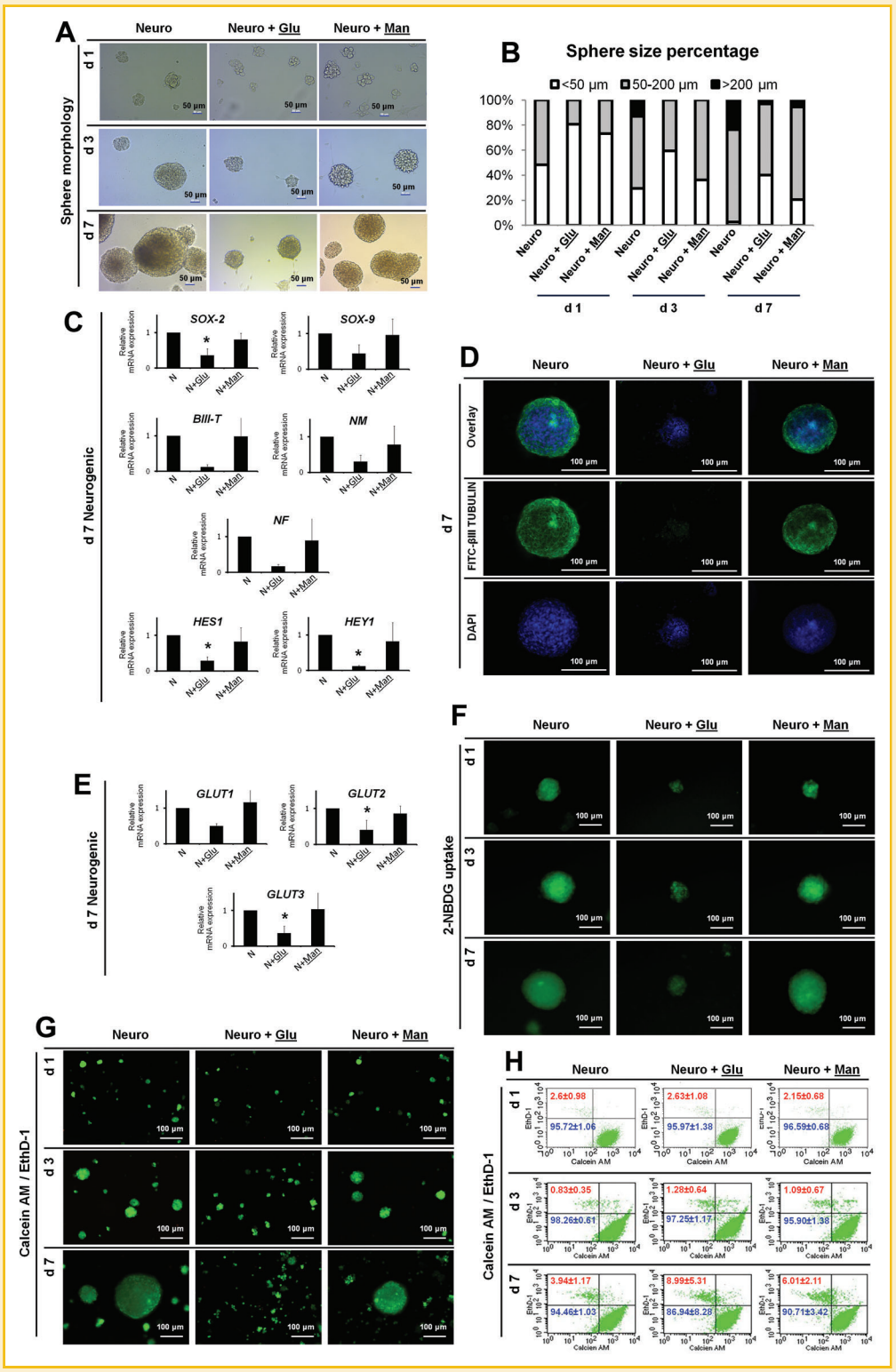

Fig. 3. High glucose condition suppressed neurosphere formation by hPDLSCs. The sphere morphology of cell cultured in normal neuroinduction condition (Neuro), high glucose neuroinduction medium (Neuro + Glu), and high mannose neuroinduction medium (Neuro + Man) was illustrated (A). The graph representing the percentage of sphere size was shown (B). Neurogenic marker gene expression was evaluated using qRT-PCR. The graphs illustrated the relative mRNA expression normalized to 18S and the control (C). Immunocytochemistry staining demonstrated βIII-TUBULIN protein expression was shown (D). *GULTs* mRNA levels were determined using qRT-PCR and the graphs represented the relative mRNA expression normalized to 18S and the control (E). The fluorescent glucose analogue, 2-NBDG, was employed to determine the cellular glucose uptake (F). Cell viability was evaluated using calcein AM/EthD-1 and further analyzed using fluorescence microscopy (G) as well as flow cytometry (H). Asterisks indicated the statistical significance compared to the normal condition (Neuro).

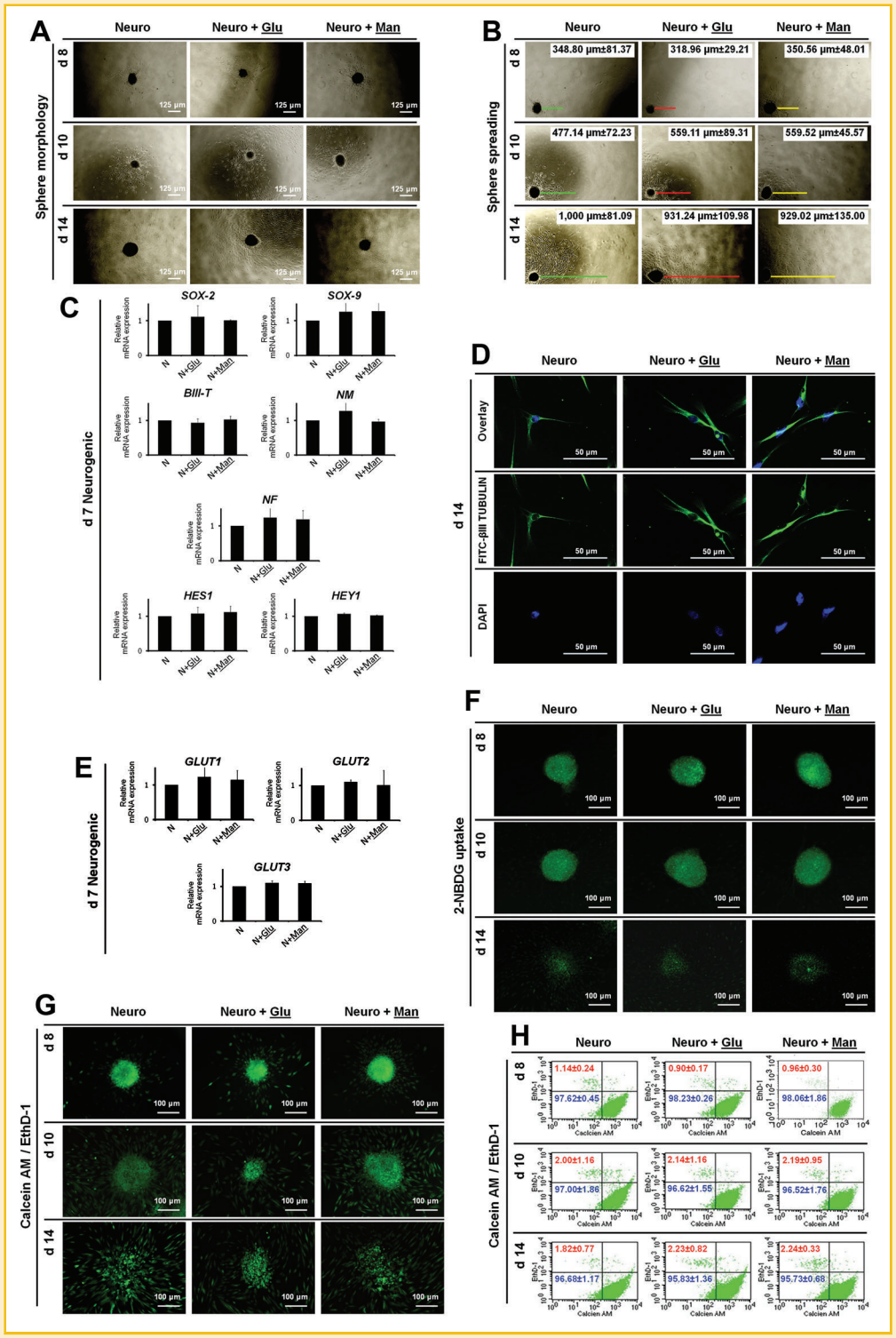

Fig. 4. Normal hPDLSCs-derived neurospheres underwent neuronal maturation even in high glucose condition. The hPDLSCs-derived neurospheres obtained from normal induction protocol were seeded into Collagen IV-coated culture dishes and underwent maturation stage in three different conditions; normal condition (Neuro), high glucose condition (Neuro + Glu), and high mannose condition (Neuro + Man). Sphere morphology (A) and sphere spreading diameter (B) were evaluated at days 1, 3, and 7. qRT-PCR was employed to illustrate the neurogenic marker gene expression and the relative mRNA expression was calculated (C). Immunocytochemistry staining for βIII-TUBULIN was evaluated at day 7 (D). *GULTs* mRNA levels were determined using qRT-PCR and the graphs represented the relative mRNA expression normalized to 18S and the control (E). The glucose uptake assay was performed using the fluorescent glucose analogue, 2-NBDG (F). Cell viability was evaluated using calcein AM/EthD-1 and further analyzed using fluorescence microscopy (G) as well as flow cytometry (H).

downregulation of *GLUTs* expression, implying the regulation via the alteration of glucose uptake. To investigate the proposed mechanism, cytochalasin B was supplemented in normal neurogenic condition to inhibit glucose uptake. The cytochalasin B at concentration of 10 μM did not have the effect on cell viability and proliferation as determined by MTT assay at days 1, 3, and 7 (data not shown). In neurosphere formation assay, the spheres in neurogenic medium supplemented with cytochalasin B (Neuro + cytochalasin B) appeared smaller in size than the normal condition (Neuro) and the percentage of small-size neurospheres (<50 μm) was increased compared to the control (Fig. 5A,B). However, the statistical significant difference in average sphere diameter was not observed (data not shown). In addition, the attenuation of neurogenic mRNA levels was observed in cytochalasin B treated group. However, the significant difference was noted for *SOX-2*, *βIII-T*, *NM*, *HES1*, and *HEY1* mRNA expression (Fig. 5C). Correspondingly, the βIII-TUBULIN protein expression in the spheres was markedly downregulated in cytochalasin B treated group (Fig. 5D).

The *GLUTs* mRNA levels (*GLUT1*, *GLUT2*, and *GLUT3*) were not different between cytochalasin B treated group and the control (Fig. 5E). However, the intracellular glucose levels were markedly reduced, comfirming the efficiency function of cytochalasin B to prevent glucose uptake (Fig. 5F). No influence of cytochalasin B on cell viability was noted (Fig. 5G,H). Together, the results illustrated that blocking of cellular glucose uptake during neurosphere formation caused the impairment of neurosphere formation by hPDLSCs.

DISCUSSION

In this study, we described the effects of high glucose conditions on hPDLSCs′ neurosphere formation and neuronal maturation. The results illustrated the deleterious effects of high glucose condition during neurosphere formation but not for neuronal maturation stage. The inhibition of glucose uptake resulted in the defective neurosphere formation by these cells.

Many publications have suggested a crucial role of glucose on stem cell functions and properties. For ES cell-derived EB formation, Mochizuki et al. [2011] have suggested that three different glucose conditions (5.5, 25, and 45 mM) but not for glucose-free condition were able to form mouse ES cell-derived EB in similar morphology and pluripotent marker expression pattern. Moreover, the glucose at concentration of 25 mM showed a beneficial role in generation of beating cardiac muscle-like clusters, but it was not suitable to form βIII-tubulin-positive neuronal cells from mouse ES-derived EB [Mochizuki et al., 2011]. Additionally, in vitro OGD condition has illustrated the sensitivity of developing or immature hippocampal neurons [Jiang et al., 2004]. It has also been shown that bone marrow-derived mesenchymal stem cells maintained in glucose reduction condition could utilize energy efficiently and showed high self-renewal and anti-replicative senescence capabilities [Lo et al., 2011]. Taken together, these reports suggested a crucial and sensitive role of glucose on cellular properties, especially in cell differentiation. For hPDLSCs, we previously reported that hPDLSCs could efficiently differentiate into functional neuronal cells in 25 mM glucose employing two-stage neurogenic induction protocol [Osathanon et al., 2013a]. In order to clarify the effects of high glucose on hPDLSCs-derived neuronal differentiation, the concentration at 125 mM was employed. In addition, this concentration did not have any effects on hPDLSCs proliferation and survival.

We observed in the present study that hPDLSCs expressed the detectable baseline levels of several neurogenic marker genes in undifferentiated stage. This may be due to the neural crest origin of periodontal ligament tissue, hence, there are some remained subpopulation of neural crest-derived cells [Kaku et al., 2012]. Thus, the intrinsic characters of neuroectodermal lineage may remain in those cell populations [Dangaria et al., 2011; Tomokiyo et al., 2012]. We noted the *βIII-TUBULIN* mRNA expression but the protein expression was observed in undifferentiated hPDLSCs. Correspondingly, Keeve et al. was also reported and hypothesized that this phenomenon may be controlled by miRNA-translation repression, resulting in absent βIII-TUBULIN protein expression [Keeve et al., 2013].

Physical properties of high glucose medium were first hypothesized as a cause of the defect in neurosphere formation. However, no difference physical factor was observed in high glucose medium compared to the normal culture medium, including the medium density and viscosity. To evaluate the influence of high osmolarity on cell behaviors, the D-mannose was supplemented in the culture medium to obtain similar concentration to those of high glucose condition. The hPDLSCs′ neurospheres formed in high mannose group were quite similar to the control, suggesting the irrelevance of high osmolarity effect on neurosphere formation impairment occurred in high glucose condition. Further investigations illustrated interesting cellular responses in high glucose condition during neurosphere formation. Comparing with normal and mannose group, the down-regulation of glucose transporters (*GLUTs*) mRNA expression and the decrease intracellular glucose in hPDLSCs-derived neurospheres were found in high glucose condition. Contrastingly, the levels of *GLUTs* genes expression and glucose uptake of hPDLSCs-derived neuronal cells during maturation stage were not different among those groups. Thus, the downregulation of *GLUTs* genes and deprivation of cellular glucose uptake might play a pivotal role in aberrations of hPDLSCs-derived neurosphere formation in such condition.

In the present study, we explored four main types of class I transporter which are classical types [Wood and Trayhurn, 2003; Adekola et al., 2012]. The *GLUT1*, *GLUT2*, and *GLUT3* mRNAs were expressed in hPDLSCs-derived neurospheres and neuronal cells, while *GLUT4* mRNA expression was absent. Moreover, the expressions of *GLUT1* and *GLUT3* mRNAs in undifferentiated hPDLSCs were noted (unpublished data). GLUT1 is widespread transporter responsible for general basal glucose transport [Carruthers et al., 2009]. Besides, GLUT3 is transporter highly expressed in neurons helping in neuronal glucose uptake and formerly designated as neuronal GLUT [Simpson et al., 2008]. The expression of *GLUT3* mRNA in undifferentiated hPDLSCs may cause by the intrinsic characteristics of neuroectodermal lineage. Regarding the down-regulation of *GLUTs* mRNA in hPDLSCs-derived neurospheres under high glucose condition, it implies the GLUT′s involvement in cellular response to high glucose conditions. GLUT1 is classified as one of

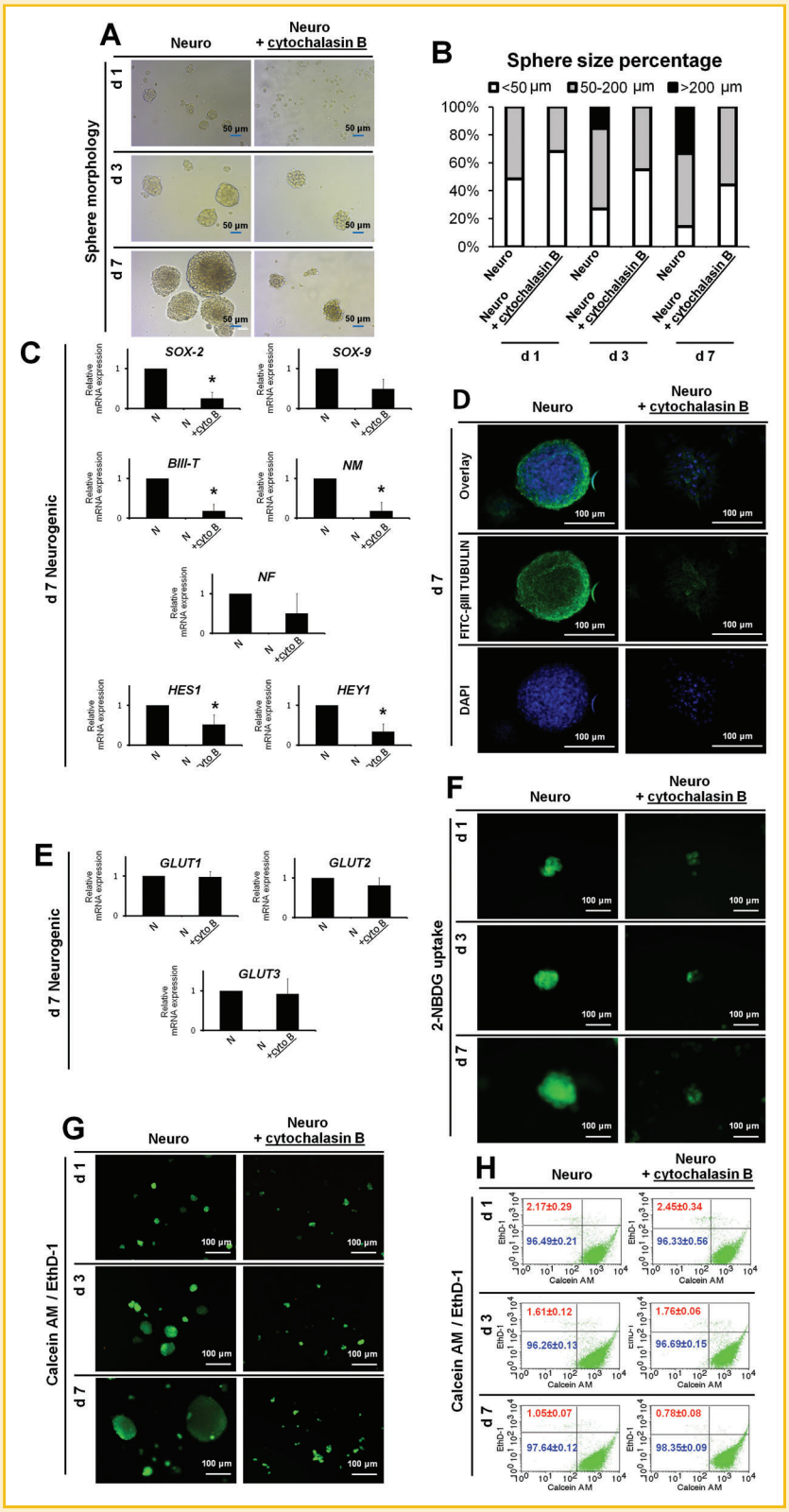

Fig. 5. Cytochalasin B attenuated neurosphere formation by hPDLSCs. The hPDLSCs were maintained in the normal neuroinduction medium (Neuro) or the neuroinduction medium supplemented with cytochalasin B (Neuro + cytochalasin B). The sphere morphology (A) and the percentage of sphere's size (B) were evaluated. The neurogenic mRNA expression was determined using qRT-PCR and the relative mRNA expression was normalized to 18S and the control (C). The βIII-TUBULIN expression was determined using immunocytochemistry staining (D). The *GLUTs* mRNA levels were determined using qRT-PCR (E). The levels of cellular glucose uptake were evaluated by fluorescent glucose analogue, 2-NBDG (F). Cell viability was evaluated using calcein AM/EthD-1 and further analyzed using fluorescence microscopy (G) as well as flow cytometry (H). Asterisks indicated the statistical significance compared to the normal condition (Neuro).

glucose-regulated proteins (GRPs) which responses to various cellular stress [Wertheimer et al., 1991; Sasson et al., 1997]. It has been shown that expression of *GLUT1* in mRNA and protein level is down-regulated in environment containing high level of hexose sugar, while glucose deprivation causes upregulation of these components [Hahn et al., 1998a,b; Itani et al., 2003; Joyner and Smoak, 2004]. Moreover, previous publications have demonstrated the mechanisms of GLUT1 expression in response to ambient glucose concentration. High glucose induced downregulation of GLUT1 via Akt pathway which was activated by PKC-oxidative stress signaling as showed in retinal pigment epithelial (RPEs) cells [Kim et al., 2007], while PKA and cAMP could upregulate GLUT1 expression by stimulation of CREB/CBP/TORC2 complex formation via NF-κB which enhanced glucose uptake and proliferation in mouse ES cells [Kim et al., 2012]. In addition, expression of GLUT3 depends on neuronal activity and glucose utilization [Vannucci et al., 1998]. Moreover, it has been shown that cAMP is involved in GLUT3 expression as illustrated in model using breast cancer cell line [Meneses et al., 2008]. In the respect of GLUT2 expression, *GLUT2* mRNA levels were upregulated upon neurogenic differentiation of hPDLSCs, while an absence of *GLUT2* mRNA was observed in undifferentiated hPDLSCs (unpublished data). GLUT2 is bidirectional transporter responsible for glucose sensor and mainly distributed in pancreatic β-cells, hepatocytes and neurons [Thorens, 2003; Scheepers et al., 2004; Leturque et al., 2009]. In addition, absent of *GLUT4* mRNA expression in undifferentiated and neurogenic differentiated hPDLSCs was observed correlating to previous publications illustrating the expression of GLUT4 in insulin-responsive tissues, for example, adipocytes and myocytes [Wood and Trayhurn, 2003; Scheepers et al., 2004; Leto and Saltiel, 2012].

It should be noted in the present study that the GLUTs expression was determined only in mRNA levels and only one time point was evaluated. Therefore, the GLUTs regulation in neurogenic differentiation by hPDLSCs should be interpreted with caution. It has been demonstrated that high glucose condition attenuated the GLUTs protein expression but not altered the mRNA levels, resulting in the decreased cellular glucose uptake [Alpert et al., 2002; Fernandes et al., 2004; Rosa et al., 2009]. The phenomenon occurred to avert the increase oxidative stress from extravagant glucose influx, implying the crucial protective role of the regulation of GLUT expression in cell behaviors [Rosa et al., 2009, 2011]. The change of mRNA expression of *GLUTs* is not enough to indicate their participation in this phenomenon. In addition, the change of GLUT expression levels may involve in other mechanisms not directly related to neurosphere formation. Therefore, the complex regulation mechanism of *GLUTs* on protective role and neurogenic differentiation is indeed needed further investigation.

Despite the issues discussed above, the influence of the alteration of glucose uptake on hPDLSCs neurosphere formation was further determined using cytochalasin B treatment condition in normal neurogenic induction condition. According with a decreased cellular glucose uptake without any change in *GLUTs* genes expression, the observations revealed a substantial effect of glucose uptake deprivation on defects of hPDLSCs-derived neurosphere formation. In addition, cell viability assay suggested the high proportion of living cells in all experimental groups, illustrating that osmotic- or stress-induced cell death might not be a main cause of neurosphere formation defects occurred in high glucose condition.

Another limitation of the present study is the lack of function study. We illustrated that the high glucose condition did not influence during the maturation step of neurogenic differentiation by hPDLSCs as determined by neurogenic marker gene and protein expression. The confirmation of the mature neurogenic function is still necessitated. The cell characters, which can exhibit action potential, should be further investigated by the electrophysiological assay to verify mature neuronal characteristics.

In summary, we illustrated that the efficiency of neurosphere formation but not for neuronal maturation by hPDLSCs was attenuated in high glucose condition. The deprivation of glucose uptake might play a pivotal role in neurosphere formation defects. Further exploration regarding molecular signaling is required to elucidate the underlying mechanism and improve efficiency of neurosphere formation.

ACKNOWLEDGEMENTS

This paper is dedicated to memory of Associate Professor Sirintorn Yibchok-anun (DVM, PhD) for her contribution and discussion before her death in January 2013. This study was supported by the Ratchadapiseksomphot Endowment Fund of Chulalongkorn University (RES560530156-HR). T.O. and P.C. was supported by Government Research Fund. PP was supported by the Research Chair Grant 2012, the National Science and Technology Development Agency (NSTDA), Thailand. C.S. was supported by Chulalongkorn university graduate scholarship to commemorate the 72nd anniversary of His Majesty King Bhumibol Adulyadej and Royal Golden Jubilee Scholarship from the Thailand Research Fund.

AUTHOR DISCLOSURE STATEMENT

No benefit of any kind will be received either directly or indirectly by the author(s). No competing financial interests exist.

REFERENCES

Adekola K, Rosen ST, Shanmugam M. 2012. Glucose transporters in cancer metabolism. Curr Opin Oncol 24:650–654.

Alpert E, Gruzman A, Totary H, Kaiser N, Reich R, Sasson S. 2002. A natural protective mechanism against hyperglycaemia in vascular endothelial and smooth-muscle cells: Role of glucose and 12-hydroxyeicosatetraenoic acid. Biochem J 362:413–422.

Carruthers A, DeZutter J, Ganguly A, Devaskar SU. 2009. Will the original glucose transporter isoform please stand up! Am J Physiol Endocrinol Metab 297:E836–E848.

Dangaria SJ, Ito Y, Luan X, Diekwisch TG. 2011. Differentiation of neural-crest-derived intermediate pluripotent progenitors into committed periodontal populations involves unique molecular signature changes, cohort shifts, and epigenetic modifications. Stem Cells Dev 20:39–52.

Egusa H, Sonoyama W, Nishimura M, Atsuta I, Akiyama K. 2012. Stem cells in dentistry—Part I: Stem cell sources. J Prosthodont Res 56:151–165.

Fernandes R, Carvalho AL, Kumagai A, Seica R, Hosoya K, Terasaki T, Murta J, Pereira P, Faro C. 2004. Downregulation of retinal GLUT1 in diabetes by ubiquitinylation. Mol Vis 10:618–628.

Govitvattana N, Osathanon T, Taebunpakul S, Pavasant P. 2013. IL-6 regulated stress-induced Rex-1 expression in stem cells from human exfoliated deciduous teeth. Oral Dis 19:673–682.

Grimm WD, Dannan A, Becher S, Gassmann G, Arnold W, Varga G, Dittmar T. 2011. The ability of human periodontium-derived stem cells to regenerate periodontal tissues: A preliminary in vivo investigation. Int J Periodontics Restorative Dent 31:e94–e101.

Hahn T, Barth S, Hofmann W, Reich O, Lang I, Desoye G. 1998a. Hyperglycemia regulates the glucose-transport system of clonal choriocarcinoma cells in vitro. A potential molecular mechanism contributing to the adjunct effect of glucose in tumor therapy. Int J Cancer 78:353–360.

Hahn T, Barth S, Weiss U, Mosgoeller W, Desoye G. 1998b. Sustained hyperglycemia in vitro down-regulates the GLUT1 glucose transport system of cultured human term placental trophoblast: A mechanism to protect fetal development? FASEB J 12:1221–1231.

Itani SI, Saha AK, Kurowski TG, Coffin HR, Tornheim K, Ruderman NB. 2003. Glucose autoregulates its uptake in skeletal muscle: Involvement of AMP-activated protein kinase. Diabetes 52:1635–1640.

Jiang X, Mu D, Manabat C, Koshy AA, Christen S, Tauber MG, Vexler ZS, Ferriero DM. 2004. Differential vulnerability of immature murine neurons to oxygen-glucose deprivation. Exp Neurol 190:224–232.

Joyner NT, Smoak IW. 2004. In vivo hyperglycemia and its effect on Glut-1 expression in the embryonic heart. Birth Defects Res A Clin Mol Teratol 70:438–448.

Kadar K, Kiraly M, Porcsalmy B, Molnar B, Racz GZ, Blazsek J, Kallo K, Szabo EL, Gera I, Gerber G, Varga G. 2009. Differentiation potential of stem cells from human dental origin—Promise for tissue engineering. J Physiol Pharmacol 60 (Suppl7):167–175.

Kaku M, Komatsu Y, Mochida Y, Yamauchi M, Mishina Y, Ko CC. 2012. Identification and characterization of neural crest-derived cells in adult periodontal ligament of mice. Arch Oral Biol 57:1668–1675.

Kawanabe N, Murata S, Murakami K, Ishihara Y, Hayano S, Kurosaka H, Kamioka H, Takano-Yamamoto T, Yamashiro T. 2010. Isolation of multipotent stem cells in human periodontal ligament using stage-specific embryonic antigen-4. Differentiation 79:74–83.

Keeve PL, Dittmar T, Gassmann G, Grimm WD, Niggemann B, Friedmann A. 2013. Characterization and analysis of migration patterns of dentospheres derived from periodontal tissue and the palate. J Periodontal Res 48:276–285.

Kim DI, Lim SK, Park MJ, Han HJ, Kim GY, Park SH. 2007. The involvement of phosphatidylinositol 3-kinase/Akt signaling in high glucose-induced down-regulation of GLUT-1 expression in ARPE cells. Life Sci 80:626–632.

Kim MO, Lee YJ, Park JH, Ryu JM, Yun SP, Han HJ. 2012. PKA and cAMP stimulate proliferation of mouse embryonic stem cells by elevating GLUT1 expression mediated by the NF-kappaB and CREB/CBP signaling pathways. Biochim Biophys Acta 1820:1636–1646.

Leto D, Saltiel AR. 2012. Regulation of glucose transport by insulin: Traffic control of GLUT4. Nat Rev Mol Cell Biol 13:383–396.

Leturque A, Brot-Laroche E, Le Gall M. 2009. GLUT2 mutations, translocation, and receptor function in diet sugar managing. Am J Physiol Endocrinol Metab 296:E985–E992.

Li X, Gong P, Liao D. 2010. In vitro neural/glial differentiation potential of periodontal ligament stem cells. Arch Med Sci 6:678–685.

Lo T, Ho JH, Yang MH, Lee OK. 2011. Glucose reduction prevents replicative senescence and increases mitochondrial respiration in human mesenchymal stem cells. Cell Transplant 20:813–825.

Maciver NJ, Jacobs SR, Wieman HL, Wofford JA, Coloff JL, Rathmell JC. 2008. Glucose metabolism in lymphocytes is a regulated process with significant effects on immune cell function and survival. J Leukoc Biol 84:949–957.

Meneses AM, Medina RA, Kato S, Pinto M, Jaque MP, Lizama I, Garcia Mde L, Nualart F, Owen GI. 2008. Regulation of GLUT3 and glucose uptake by the cAMP signalling pathway in the breast cancer cell line ZR-75. J Cell Physiol 214:110–116.

Mi HW, Lee MC, Fu E, Chow LP, Lin CP. 2011. Highly efficient multipotent differentiation of human periodontal ligament fibroblasts induced by combined BMP4 and hTERT gene transfer. Gene Ther 18:452–461.

Mochizuki H, Ohnuki Y, Kurosawa H. 2011. Effect of glucose concentration during embryoid body (EB) formation from mouse embryonic stem cells on EB growth and cell differentiation. J Biosci Bioeng 111:92–97.

Mrozik K, Gronthos S, Shi S, Bartold PM. 2010. A method to isolate, purify, and characterize human periodontal ligament stem cells. Methods Mol Biol 666:269–284.

Nowwarote N, Osathanon T, Jitjaturunt P, Manopattanasoontorn S, Pavasant P. 2013. Asiaticoside induces type I collagen synthesis and osteogenic differentiation in human periodontal ligament cells. Phytother Res 27:457–462.

Osathanon T, Nowwarote N, Pavasant P. 2011. Basic fibroblast growth factor inhibits mineralization but induces neuronal differentiation by human dental pulp stem cells through a FGFR and PLCgamma signaling pathway. J Cell Biochem 112:1807–1816.

Osathanon T, Manokawinchoke J, Nowwarote N, Aguilar P, Palaga T, Pavasant P. 2013a. Notch signaling is involved in neurogenic commitment of human periodontal ligament-derived mesenchymal stem cells. Stem Cells Dev 22:1220–1231.

Osathanon T, Ritprajak P, Nowwarote N, Manokawinchoke J, Giachelli C, Pavasant P. 2013b. Surface-bound orientated Jagged-1 enhances osteogenic differentiation of human periodontal ligament-derived mesenchymal stem cells. J Biomed Mater Res A 101:358–367.

Rosa SC, Goncalves J, Judas F, Mobasheri A, Lopes C, Mendes AF. 2009. Impaired glucose transporter-1 degradation and increased glucose transport and oxidative stress in response to high glucose in chondrocytes from osteoarthritic versus normal human cartilage. Arthritis Res Ther 11: R80.

Rosa SC, Rufino AT, Judas FM, Tenreiro CM, Lopes MC, Mendes AF. 2011. Role of glucose as a modulator of anabolic and catabolic gene expression in normal and osteoarthritic human chondrocytes. J Cell Biochem 112:2813–2824.

Sasson S, Kaiser N, Dan-Goor M, Oron R, Koren S, Wertheimer E, Unluhizarci K, Cerasi E. 1997. Substrate autoregulation of glucose transport: Hexose 6-phosphate mediates the cellular distribution of glucose transporters. Diabetologia 40:30–39.

Scheepers A, Joost HG, Schurmann A. 2004. The glucose transporter families SGLT and GLUT: Molecular basis of normal and aberrant function. J Parenter Enteral Nutr 28:364–371.

Seo BM, Miura M, Gronthos S, Bartold PM, Batouli S, Brahim J, Young M, Robey PG, Wang CY, Shi S. 2004. Investigation of multipotent postnatal stem cells from human periodontal ligament. Lancet 364:149–155.

Simpson IA, Dwyer D, Malide D, Moley KH, Travis A, Vannucci SJ. 2008. The facilitative glucose transporter GLU T3: 20 years of distinction. Am J Physiol Endocrinol Metab 295:E242–E253.

Song JS, Kim SO, Kim SH, Choi HJ, Son HK, Jung HS, Kim CS, Lee JH. 2012. In vitro and in vivo characteristics of stem cells derived from the periodontal ligament of human deciduous and permanent teeth. Tissue Eng Part A 18:2040–2051.

Techawattanawisal W, Nakahama K, Komaki M, Abe M, Takagi Y, Morita I. 2007. Isolation of multipotent stem cells from adult rat periodontal ligament by neurosphere-forming culture system. Biochem Biophys Res Commun 357:917–923.

Thorens B. 2003. A gene knockout approach in mice to identify glucose sensors controlling glucose homeostasis. Pflugers Arch 445:482–490.

Tomokiyo A, Maeda H, Fujii S, Monnouchi S, Wada N, Kono K, Yamamoto N, Koori K, Teramatsu Y, Akamine A. 2012. A multipotent clonal human periodontal ligament cell line with neural crest cell phenotypes promotes

neurocytic differentiation, migration, and survival. J Cell Physiol 227:2040–2050.

Vannucci SJ, Clark RR, Koehler-Stec E, Li K, Smith CB, Davies P, Maher F, Simpson IA. 1998. Glucose transporter expression in brain: Relationship to cerebral glucose utilization. Dev Neurosci 20:369–379.

Wertheimer E, Sasson S, Cerasi E, Ben-Neriah Y. 1991. The ubiquitous glucose transporter GLUT-1 belongs to the glucose-regulated protein family of stress-inducible proteins. Proc Natl Acad Sci USA 88:2525–2529.

Wood IS, Trayhurn P. 2003. Glucose transporters (GLUT and SGLT): Expanded families of sugar transport proteins. Br J Nutr 89:3–9.

SUPPORTING INFORMATION

Additional supporting information may be found in the online version of this article at the publisher's web-site.